α7 nicotinic receptor full agonist reverse basolateral amygdala hyperactivity and attenuation of dopaminergic neuron activity in rats exposed to chronic mild stress

Gilda A. Neves[*], **Anthony A. Grace**

Departments of Neuroscience, Psychiatry and Psychology, University of Pittsburgh, A210 Langley Hall, Pittsburgh, PA, 15260, USA

Abstract

Neuroimaging and preclinical studies showing that nicotinic receptors (nAChR) may play a role in mood control has increased interest in targeting the cholinergic system for treatment of major depressive disorder. Indeed, modulation of nAChRs in the basolateral amygdala (BLA) are sufficient to produce an anti-immobility effect in the mouse tail suspension test. However, how α7 nAChR modulation impacts BLA neuronal activity *in vivo* as well as the downstream mechanisms involved in its mood-related effects are not understood. In this work, we used the unpredictable chronic mild stress (CMS) model to investigate the mechanisms underlying the antidepressant-like effect of an α7 nAChR full agonist on BLA-induced changes in dopaminergic neurotransmission. Male adult Sprague-Dawley rats were exposed to four weeks of CMS. Behavioral and electrophysiological experiments were performed within one week following stress. CMS exposure increase rats' immobility time in the forced swimming test, decreased the number of spontaneously active dopamine neurons in the ventral tegmental area and increased the firing rate of putative projection neurons in the BLA. Stress-induced behavioral and electrophysiological changes were reversed by a single systemic administration of PNU282987. In summary, our findings corroborate previous descriptions of a potential rapid antidepressant effect for the α7 nAChR full agonist. This effect appears to involve a mechanism distinct from those of classic antidepressants: normalization of BLA hyperactivity and, consequently, of DA hypofunction. These observations corroborate the role of α7 nAChR as a potential target for novel antidepressant drug development.

[*]Corresponding author current address: Gilda A. Neves, Instituto de Ciências Biomédicas, Universidade Federal do Rio de Janeiro, Av. Carlos Chagas Filho, 373, bloco J, sala J1-021, Cidade Universitária, Rio de Janeiro, RJ, Brazil, Phone: +55-21-2280-4694, ganeves@icb.ufrj.br.

Keywords

α7 nicotinic receptor; electrophysiology; chronic mild stress; basolateral amygdala; ventral tegmental area; dopamine

1. Introduction

Since the serendipitous discovery of psychotherapeutic drugs, the monoaminergic hypothesis of major depressive disorder (MDD) has dominated drug development. Despite the substantial number of antidepressants available, only 30% of MDD patients remitted with the first drug tested, with a final total rate of remission of 67% (Rush et al., 2006). A major advance in MDD treatment was achieved only recently with the description of the rapid antidepressant effects of scopolamine (Furey and Drevets, 2006) and ketamine (Zarate Jr et al., 2006), highlighting the importance to look beyond monoamines for searching new fast-acting drugs targeting treatment-resistant patients.

Cholinergic system involvement in the pathophysiology of MDD was first postulated based on the induction of depression symptoms by acetylcholinesterase inhibitor insecticides (Janowsky et al., 1972). Although post-mortem studies failed to demonstrate consistent changes in the cholinergic system in depressed patients (Dagytė et al., 2011), neuroimaging data showed increased choline levels in acutely depressed patients and its reversal after symptom recovery (Steingard et al., 2000) as well as increased acetylcholine levels (Hannestad et al., 2013) and decreased availability of β2-containing nicotinic receptors (nAChR) (Saricicek et al., 2012). Furthermore, there is a high prevalence of nicotine use among depressed patients (50–60%), smoking cessation has been related to anxiety and depression symptoms (Glassman et al., 1990) and nicotine transdermal patches were shown to improve symptoms in MDD patients without smoking history (Salín-Pascual et al., 1996). Therefore, changes in cholinergic neurotransmission and, more specifically, nAChRs may underlie mood imbalances and be an effective target for treatment.

Animal studies provided further support to this hypothesis. Systemic administration of the acetylcholinesterase inhibitor physostigmine increased the immobility time in both forced swim and tail suspension tests, and this effect was blocked by the non-selective nicotinic receptor antagonist mecamylamine (Mineur et al., 2013; 2018). Moreover, nicotine administration induced an antidepressant-like effect in rodents (Andreasen and Redrobe, 2009; Andreasen et al., 2011; Biala et al., 2017; Tizabi et al., 1999; Xiao et al., 2017) that was reproduced by mecamylamine (Andreasen and Redrobe, 2009). Mecamylamine was inactive in mice lacking α7 or β2 subunits of nAChRs (Rabenstein et al., 2006) and selective antagonists of both α7 or α4β2 nAChR also induced anti-immobility effects (Andreasen et al., 2009, Mineur et al., 2018) implying both subtypes of nAChR in mood control. Moreover, nonselective blockade of nAChRs in the basolateral amygdala (BLA) appears to be sufficient to induce an anti-immobility effect and knocking down α7 or β2 subunits in the BLA also reduced the immobility time in the tail suspension test (Mineur et al., 2016), confirming a role for this brain area in the antidepressant-like effect of nicotinic drugs.

However, the consequences of BLA nAChR blockade/desensitization as well as the brain regions involved downstream in the observed effects are unknown.

The BLA is a main component of the limbic system involved in the control of affective behaviors, having a pivotal role in fear and stress related responses (Prager et al., 2016). Amygdala hyperactivity was detected in depressed patients (Fales et al., 2008) and chronic stress models of depression (Zhang and Rosenkranz, 2012; 2016). This hyperactivity disturbs the function of several brain regions involved in motivation, anxiety, fear and cognition, such as the nucleus accumbens, prefrontal cortex and ventral pallidum (VP) (Sharp et al., 2017). Previous data from our group showed that rats chronically exposed to unpredictable stress or to the learned helplessness model develop a hypodopaminergic state characterized by a decrease in the number of spontaneously active dopamine (DA) neurons in the reward-related ventral tegmental area (VTA) (Belujon and Grace, 2014; Chang and Grace, 2014; Moreines et al., 2017, Rincón-Cortés and Grace, 2017). This reduction is abolished by BLA inactivation, implicating a putative hyperactivity of this brain region in stress-induced inhibition of DA neurons (Chang and Grace, 2014). Moreover, local infusion of an α7 nAChR full agonist into the BLA increases the number of spontaneously active DA neurons in the reward-related VTA in normal rats (Neves and Grace, 2018), pointing to the involvement of this brain circuit in the moodregulating function of α7 nAChRs.

In this work, we aimed to investigate the potential involvement of the BLA-VTA interplay in the mechanism of the antidepressant-like effect of an α7 nAChR full agonist. Most studies conducted with nAChR selective ligands used naïve mice or animals exposed to stress for a short period of time (Andreasen et al., 2009; Mineur et al., 2016; 2018); however, chronic stress is one of the major contributing factors for MDD development (Hammen, 2005). Considering the different outcomes induced by chronic and acute stress in brain and behavior (Gill and Grace, 2013; Valenti et al., 2012; Zhang and Rosenkranz, 2012), we demonstrated initially the α7 nAChR full agonist anti-immobility effect following chronic unpredictable mild stress, a model of anhedonia and depression-related phenotypes (Willner, 2016). The potential of the α7 nAChR agonist to counteract the stress-induced electrophysiological changes in both VTA DA and BLA neurons was then investigated.

2. Experimental procedures

2.1. Animals

Male adult Sprague-Dawley rats (n = 127, 300–315 g, PND65) were pair-housed for 5 days at constant room temperature (22°C) and humidity (47%) under a 12h light-dark cycle (lights off at 7:00 pm), with food and water available ad libitum. Protocols were performed according to National Institute of Health Guide for the Care and Use of Laboratory Animals and were approved by the Institutional Animal Care and Use Committee of the University of Pittsburgh.

2.2. Unpredictable Chronic Mild Stress (CMS)

The unpredictable chronic mild stress protocol was conducted as previously described (Stedenfeld et al., 2014) and adapted by us (Chang & Grace, 2014). Briefly, rats were single

housed and exposed randomly to 3–4 stressors/week for 4 weeks, including: food deprivation overnight, water deprivation overnight, reversal dark-light cycle over the weekend, damp bedding, cage tilting, white noise (~90dB), strobe light, foreign intruder and predator odor. Control rats matched by age and weight were kept double housed in standard conditions essentially undisturbed for the same amount of time. Weight gain was monitored weekly. All behavioral and electrophysiological experiments were conducted at most 7 days after stress interruption (Fig. 1A). Three cohorts of animals were used: one for behavioral assays, a second for VTA recordings and the third for BLA recordings.

2.3. Behavioral Tasks

2.3.1. Forced swimming test—
The protocol originally described by Porsolt and coworkers (1978) was employed with minor modifications (Rincón-Cortés and Grace, 2017). Rats were exposed to the forced swim test (FST) in transparent plexiglas cylinders (50cm height, 20cm diameter, water at 30cm, 23–25°C) twice. Swimming sessions lasted 15min and 5min, with 24h interval. The room was kept at 23 ± 2°C under artificial lighting. Immobility time was measured by a trained observer blind to treatment condition. A rat was considered immobile when it remained floating making only the movements necessary to keep its head above the water. All swimming sessions occurred between 8 a.m. and 1 p.m. Drug treatment was performed 35min before the second swimming session (Fig. 1B).

2.3.2. Locomotor activity—
Rat locomotion was assessed in an automated rectangular ($70 \times 30 \times 40$ cm) chamber by the total distance traveled in a 5min period. The number of horizontal beam breaks were detected and transformed by TrueScan software (Coulbourn Instruments). Locomotor activity was evaluated immediately before the second swimming session (30min after drug) (Fig. 1B).

2.4. Electrophysiology

Animals were anesthetized with chloral hydrate (400mg/kg i.p. supplemented when necessary), placed in a stereotaxic apparatus and their body temperature was maintained at 37°C using a thermostatically-controlled heating pad. Single-unit extracellular recordings were performed with single glass microelectrodes (6–8MΩ) filled with 2% Chicago sky blue dye dissolved in 2M NaCl. Spontaneously active neurons were recorded with open filter settings (high pass=10Hz; low pass=10kHz). Drug was administered through the lateral tail vein 15 min before recordings.

Dopaminergic neurons were recorded by lowering electrodes into the VTA (AP=−5.3 to −5.7mm, ML=−0.6 to −1.0mm, VD=+6.5 to +9.0mm). Population activity was determined by performing 6–9 consecutive vertical electrode tracks through the VTA separated by 200μm in a preset pattern (figure 1c). DA neurons were identified based on location, firing rate and pattern and waveform as previously described (Grace and Bunney, 1983; Ungless and Grace, 2012). Activity of each DA neuron was recorded for at least 1min. Three properties were analyzed: population activity (number of active DA neurons per electrode track), firing rate and percentage of action potentials occurring in bursts. Burst initiation was defined as the occurrence of two spikes with an interspike interval 80 ms, and the termination was set as the occurrence of a subsequent interspike interval >160ms (Grace and

Bunney, 1984). To determine the medial-lateral distribution of the VTA DA neurons recorded, data were analyzed according to electrode placement as previously described (Lodge and Grace, 2012; Neves and Grace, 2018) (Fig. 1C).

For BLA neuron recordings, electrodes were lowered (AP=−2.8 to −3.2mm, ML=−4.5 to −4.9mm, VD=+6.0 to +8.5mm) and six vertical electrode tracks separated by 200μm were performed per rat. Each isolated neuron was recorded for at least 3min. Location of the recorded neurons was confirmed by coordinates reconstructed based on histological confirmation of electrode placement (Fig. 1D). Putative projection neurons and interneurons were separated based on firing rate and action potential half-width criteria. For projection neurons, only those with firing rate <1Hz were included in the analysis (Du and Grace, 2016; Likhtik et al., 2006; Rosenkranz and Grace, 1999). Since action potential characteristics can change according to filter settings and electrode type, a half-width criteria was established by fitting the frequency distribution of half-width values from our control group into two gaussian non-linear regressions as previously described (Zhang and Rosenkranz, 2016). Two properties were analyzed: proportion of neurons active (number of a specific type of neuron/total number of neurons recorded) and firing rate (Hz).

After recording, the electrode site was marked via electrophoretic ejection of Chicago sky blue dye (−20μA for 20–30min). Animals were euthanized by anesthetic overdose and decapitated. Brains were removed, fixed in 8% paraformadehyde in 0.2M PBS and cryoprotected in 25% sucrose in 0.2M PBS. Sixty μm sections through the extent of the VTA and BLA were stained with a mix of 95% Neutral Red and 5% Cresyl Violet for verification of electrode placements (Fig. 1C and 1D).

2.5. Drug

PNU 282987 is a high affinity ($K_d = 220$ nM) full agonist of α7 nAChR, showing an EC_{50} for receptor activation of 110 nM (Arunrungvichian et al., 2015). It has negligible affinity for β2-containing nAChR since at 1 μM it can only displace 14% of cytisine binding from rat brain (Bodnar et al., 2005). PNU282987 hydrate (Sigma-Aldrich) was dissolved in saline (0.9% NaCl). Controls received saline at 1mL/kg body weight. All solutions were made immediately before treatment. PNU282987 dose (1mg/kg) was selected based on previous data (Neves and Grace, 2018). Drug and saline were administered by the intraperitoneal rout before behavioral experiments and intravenously (using the lateral tail vein) before electrophysiological recordings.

2.6. Data analysis

Electrophysiological data of neuron activity states and action potential properties were collected and analyzed using Powerlab LabChart (ADInstruments) and NeuroExplorer (NexTech Systems) software. Frequency distribution of the BLA neuron action potential half-width was analyzed using non-linear regression to fit a one or sum of two gaussian curves model. Best data fit was evaluated by the extra sum-of-squares F-test. Weight gain and forced swim immobility of the same animals across time were analyzed using a two-way repeated measures ANOVA, with stress (control and CMS) as the independent factor and time point as the repeated factor. According to the number of experimental groups, total

forced swim immobility time was analyzed by Student's t test or two-way ANOVA, with stress and acute treatment (vehicle and PNU282987) as independent factors, as well as for VTA and BLA electrophysiological data (number of DA neurons per track, firing rate, percentage of spikes in bursts, proportion of neurons). All post-hoc analysis was performed using the Bonferroni test. Firing rate distributions were compared using the Kolmogorov-Smirnov test. Statistics were calculated using SigmaStat (Jandel Scientific Corporation). Data are expressed as mean ± S.E.M. and differences were considered statistically significant at $p < 0.05$.

3. Results

3.1. PNU282987 has anti-immobility effect in CMS rats

Both CMS and control groups gained weight equally during the experimental procedure (Fig. 2A, two-way RM ANOVA, $F_{interaction(4,240)} = 3.597$, $p = 0.007$, basal vs subsequent weeks: Bonferroni test, $p < 0.001$; control vs CMS: $p > 0.091$). Increase in immobility time of stressed animals was detected in the first swim session (Fig. 2B, control: 207±17s, CMS: 266±23s. Student's t test, t=2.078, df=60, $p = 0.042$). Data showed a gradual increase in immobility over time for both groups (Fig. 2C, two-way RM ANOVA, $F_{time(2,120)} = 152.2$, $p < 0.001$) and CMS rats show higher immobility at all time points (two-way RM ANOVA, $F_{stress(1,120)} = 4.492$, $p = 0.038$).

On the second day, the effect of a single injection of PNU282987 was evaluated. There was no difference in locomotion between groups (Fig. 2D, two-way ANOVA, $F_{stress(1,58)} = 0.032$, p=0.859; $F_{treatment(1,58)} = 0.071$, p=0.791; $F_{interaction(1,58)} = 0.881$, p=0.352). Significant differences were detected in the forced swimming test (Fig. 2E, two-way ANOVA, $F_{interaction(1,58)} = 4.990$, $p = 0.029$). Raised immobility time was still detected in CMS rats that received vehicle (control+vehicle 45±5s vs CMS+vehicle 82±9s, Bonferroni test, $p < 0.001$); however the α7 nAChR agonist induced an anti-immobility effect in CMS-exposed rats (CMS+PNU282987 55±7s, Bonferroni test, $p = 0.006$) without interfering with the behavior of controls (control+PNU282987 48±5s, Bonferroni test, $p = 0.433$).

3.2. PNU282987 reversed the decrease in VTA DA population activity induced by CMS

CMS exposure decreased the number of spontaneously active DA neurons in the VTA (Fig. 3A and 3B, two-way ANOVA, $F_{interaction(1,26)} = 9.724$, $p = 0.004$) from 1.3±0.1cells/track in controls to 0.6±0.1cells/track in CMS rats (Bonferroni test, $p < 0.001$). This decrease was detected across the VTA, being more prominent in central tracks (Fig. 3C, central region, two-way ANOVA, $F_{stress(1,26)} = 4.568$, $p = 0.042$). PNU282987 did not change the number of spontaneously active DA neurons in controls (1.2±0.1cells/track, Fig. 3A, Bonferroni test $p = 0.534$), as previously reported (Neves and Grace, 2018). However, the drug increased the number of VTA DA neurons recorded in CMS-exposed rats (1.1±0.2 cells/track, Bonferroni test $p < 0.001$) to control levels. Although not statistically significant with respect to region, this reversal appeared to occur across the medial-lateral extent of the VTA (Fig. 3C, two-way ANOVA, medial VTA: $F_{interaction(1,22)} = 3.541$, $p = 0.073$; central VTA: $F_{interaction(1,26)} = 4.190$, $p = 0.051$; lateral VTA: $F_{interaction(1,26)} = 1.386$, $p = 0.250$).

No significant differences were found in the burst pattern of DA neurons (Fig. 3D, two-way ANOVA, $F_{stress(1,235)}=1.915$, $p=0.168$; $F_{treatment(1,235)}=0.267$, $p=0.606$, $F_{interaction(1,235)}=1.515$, $p=0.220$); however, CMS rats showed an increase in the average firing rate (Fig. 3E, control+vehicle: 3.7±0.2Hz, CMS+vehicle: 5.0±0.4Hz, two-way ANOVA, $F_{interaction(1,235)}=11.428$, $p<0.001$, Bonferroni test, $p=0.004$) and a shift in the frequency distribution curve to higher values (Fig. 3F, Kolmogorov-Smirnov, D=0.328, $p=0.022$). This alteration was also reversed by PNU282987 treatment (Fig. 3E, CMS+PNU: 2.3±0.2 Hz, Bonferroni test, $p=0.002$) leading to a shift in the distribution curve to lower frequency values (Fig. 3G, Kolmogorov-Smirnov, D=0.389, $p=0.004$). The α7 nAChR agonist did not change the firing rate of DA neurons in control rats (Fig. 3E, control+PNU: 4.4±0.2Hz, Bonferroni test, $p=0.132$). The stress-induced increase in DA neuron firing rate was observed across the medial-lateral extent of the VTA (Fig. 3H) and again the most substantial effect was detected in the central tracks (two-way ANOVA, $F_{interaction(1,80)}=11.52$, $p=0.001$, control+vehicle: 3.8±0.4Hz, CMS+vehicle: 5.5±0.7Hz, Bonferroni test, $p=0.016$). However, the regional specificity in the frequency distribution between CMS and control groups only reached trend levels likely due to the comparatively smaller number of neurons analyzed (Fig. 3I, Kolmogorov-Smirnov, D=0.457, $p=0.092$). Once more the PNU282987 response could be seen in all regions of the VTA, reaching statistical significance in the central tracks (Fig. 3H, CMS+PNU: 3.5±0.4Hz, Bonferroni test, $p=0.006$). No significant difference was observed in the frequency distribution curves (Fig. 3J, Kolmogorov-Smirnov, D=0.491, $p=0.066$).

3.3. PNU282987 counteracted stress-induced BLA hyperactivity

The distribution of spike half-widths of BLA neurons was fitted to a sum of two gaussian curves, which fit better than a single gaussian (extra sum of squares F-test, $F_{(3,123)}=3.643$, $p=0.015$), allowing identification of two populations of neurons (Fig. 4A) as previously described (Zhang and Rosenkranz, 2016). The first population had a half-width of 0.29±0.06ms, while the second one exhibited 0.63±0.13ms. The curves intercept was at 0.38ms. Limits for neuron classification were calculated as average ± 2 SD for each curve (95.4% of the sample) to decrease uncertainty. This approach led to the inclusion of neurons with half-width <0.37ms as putative interneurons and >0.40ms as projection neurons (Fig. 4B and 4C). Neurons with action potential half-width between these values were excluded from the final analysis. Therefore, these two populations of neurons were analyzed separately.

Most of the BLA neurons recorded were presumptive projection neurons. Control+vehicle group showed 68 ± 9% of the neurons recorded per rat classified as projection neurons, and this proportion was not affected by stress or drug treatment (Fig. 4D, two-way ANOVA, $F_{stress(1,32)}=0.395$, $p=0.534$; $F_{treatment(1,32)}=0.037$, $p=0.849$; $F_{interaction(1,32)}=1.345$, $p=0.255$). However, projection neurons of the stress-exposed group were firing significantly faster than controls (Fig. 4E, control+vehicle: 0.26±0.03 Hz, CMS+vehicle: 0.35±0.04 Hz, two-way ANOVA, $F_{interaction(1,217)}=4.306$, $p=0.039$, Bonferroni test, $p=0.033$). The firing rate distribution showed a shift in the curve peak to higher values in stress-exposed rats (Fig. 4F, Kolmogorov-Smirnov, D=0.273, $p=0.043$). PNU282987 did not change the firing rate of neurons in control rats (Fig. 4E, 0.27±0.03 Hz, Bonferroni test, $p=0.904$) but significantly

decreased their frequency in stress-exposed animals (0.23±0.3 Hz, Bonferroni test, p=0.012). The frequency distribution curves were not significantly different (Fig. 4G, Kolmogorov-Smirnov, D=0.282, p=0.073) but showed a trend toward smaller peak values in the PNU282987-treated group.

Control+vehicle group was found to have 21 ± 7% of neurons classified as interneurons and this proportion was similar in all groups (Fig. 4H, two-way ANOVA, $F_{stress(1,32)}$=0.187, p=0.668; $F_{treatment(1,32)}$=0.069, p=0.794; $F_{interaction(1,32)}$=1.449, p=0.237). There was no significant difference in putative interneuron firing rate between groups (Fig. 4I, two-way ANOVA, $F_{stress(1,40)}$=0.007, p=0.936; $F_{treatment(1,40)}$=0.0008, p=0.977; $F_{interaction(1,40)}$=3.271, p=0.078), but a trend for a stress-induced decrease in firing rate could be seen (control+vehicle: 1.51±0.66Hz, CMS+vehicle: 0.61±0.18Hz). The stressed group treated with PNU282987 was nearly identical to control animals (1.57±0.53Hz); however, there is a trend for a reduction in the firing rate of the putative interneurons induced by the α7 nAChR agonist in controls (0.58±0.14Hz).

4. Discussion

In this work, we showed that a single administration of the α7 nAChR full agonist PNU282987 induced an anti-immobility effect in animals previously exposed to CMS but not in normal rats. Previous work investigating the effects of α7 nAChR ligands on FST or tail suspension tasks yielded conflicting results. While a lack of effect was reported in mice (Andreasen et al., 2009; 2012; Mineur et al., 2018), studies in rats showed PNU282987 anti-immobility effect only after repeated administration (Marcus et al., 2016) or at higher doses (Melis et al., 2013). However, these studies were conducted in non-stressed normal animals. Only a few studies investigated the effects of α7 nAChR selective ligands in depressionassociated phenotypes in repeatedly stressed animals. GTS-21 (an α7 nAChR partial agonist and β2-containing nAChR antagonist also known as DMXBA) reversed the behavioral changes induced by repeated restraint stress in mice after repeated treatment, and its effects were blocked by the α7 nAChR selective antagonist α-bungarotoxin (Zhao et al., 2017). Also, repeated administration of the selective α7 nAChR partial agonist SSR180711 improved CMS-exposed mouse physical care (Pichat et al., 2007). In contrast, both GTS-21 and the selective α7 nAChR antagonist metyllycaconitine failed to reverse social interaction deficits after three days of social defeat (Mineur et al., 2018). Neither of these studies utilized a single administration and most of them did not present data on a non-stressed drug-treated group. Thus, our work is the first to show that CMS animals are more sensitive to the anti-immobility effect of PNU282987 and corroborates a potential antidepressant effect of α7 nAChR full agonists after a single dose.

Accompanying the increase in FST immobility, rats exposed to CMS developed a hypodopaminergic status characterized by a decrease in the number of spontaneously active DA neurons in the VTA. This phenomenon was previously shown by our group in CMS rats (Chang and Grace, 2014; Moreines et al., 2017; Rincón-Cortés and Grace, 2017) and also in the learned helplessness model (Belujon and Grace, 2014). Dysregulation of dopamine neurotransmission has been implicated in the genesis of several MDD symptoms, including anhedonia, avolition, apathy and blunted response to rewarding stimulus (Belujon and

Grace, 2017). In fact, the decrease in VTA DA neuron population activity in animal models is corelated with behavioral changes analogous to these symptoms, such as impaired sucrose preference and higher immobility (Belujon and Grace, 2017; Tye et al., 2013). When presented with a rewarding stimulus or in anticipation of a reward, DA neurons are activated and fire bursts of action potentials (Schultz, 1997). However, only DA neurons that are spontaneously active at baseline can be driven to burst fire (Floresco et al., 2003). Thus, the decrease in VTA DA population activity can be correlated to a blunted response to a motivationally salient stimulus. Accordingly, Tye and coworkers (2013) showed that selective optogenetic activation of VTA DA neurons was able to reverse the CMS-induced increase in immobility time in the tail suspension and forced swim tasks. In our study, a single injection of PNU282987 was able to normalize VTA DA population activity in CMS-exposed rats without affecting control animals. This pattern is similar to the one induced by PNU282987 in the FST, suggesting that the increase in the number of spontaneously active DA neurons may contribute to its anti-immobility effect. CMS exposure also increased the firing rate of DA neurons, as previously reported (Bambico et al., 2019; Chang and Grace, 2014). Interestingly, PNU282987 was also able to normalize this change, confirming its potential to counteract stress-induced effects on dopaminergic transmission.

4.1. CMS exposure increases the firing rate of BLA projection neurons: reversal by PNU282987

The BLA is involved in controlling affective behaviors, having a pivotal role in fear and stress-related responses. Our work showed that CMS-exposed rats developed a persistent BLA hyperactivity characterized by an increase in the firing rate of projection neurons associated with a trend-level decrease in the firing rate of putative interneurons. Similar changes were described in animals submitted to repeated restraint stress (Zhang and Rosenkranz, 2012; 2016); however, to the best of our knowledge, this is the first description of this phenomenon in the CMS model. Chronic stress increases the number of spines and length of dendrites in BLA principal neurons (Vyas et al., 2006), their sensitivity to glutamate and the frequency of sEPSPs (Zhang and Rosenkranz, 2016); changes consistent with an enhanced excitatory drive. BLA local inhibitory circuits have a prominent role in controlling principal neuron excitability (Prager et al., 2016). Whereas parvalbumin (PV) positive neurons interact directly with the cell bodies and appear to be involved in feedback inhibition (Muller et al., 2006), calbindin-expressing interneurons appear to be involved in feedforward inhibitory mechanisms including those mediated by neurons projecting from the prefrontal cortex (Unal et al., 2015). Evidence indicates that downregulation of BLA inhibitory circuits is involved in the persistent hyperactivity of principal neurons after chronic stress. Different repeated stress paradigms reduce the levels of the GABA synthetizing enzyme glutamic acid decarboxylase (GAD) in the BLA (Ortiz et al., 2015). Moreover, chronic stress reduces the frequency of sIPSPs in principal neurons resulting in a long-lasting loss of tonic inhibitory control (Liu et al., 2014; Zhang and Rosenkranz, 2016). These observations are consistent with our results and show that complex mechanisms are involved in the inhibitory/excitatory balance leading to BLA hyperactivity after repeated stress.

A single systemic administration of PNU282987 had beneficial effects on CMS-exposed rats: it significantly reversed the hyperactivity of BLA projection neurons and appeared to attenuate the changes in putative interneuron firing rate. α7 nAChR are highly expressed in the BLA (Tribollet et al. 2004), being found at somatodentritic regions of both principal neurons and interneurons (Klein and Yakel, 2006; Pidoplichko et al., 2013) and on glutamatergic terminals (Jiang and Role, 2008). The only study describing the effects of a selective α7 nAChR agonist in BLA slices showed a higher frequency of both IPSCs and EPSCs on principal neurons and a direct depolarization and increased EPSC frequency of interneurons, leading to an overall reduction in BLA excitability (Pidoplichko et al., 2013). Thus, it is possible that PNU282987 effects on CMS-exposed rats may involve one or more of those mechanisms and, therefore, be a result of the modulation of α7 nAChR locally expressed in the BLA. However, the Pidoplichko and coworkers (2013) study was conducted in slices of non-stressed rats. While acute stress modestly increases acetylcholine release in the BLA (Mark et al., 1996), the consequences of chronic stress on cholinergic neurotransmission in this brain region require further study. Thus, changes in the BLA circuit induced by chronic stress might change the mechanisms involved in α7 nAChR mediated control of its excitability. Moreover, α7 nAChRs also impact brain regions that control BLA activity and are also affected by chronic stress, such as the hippocampus or infralimbic prefrontal cortex, and actions in these regions may also play a role in these responses.

PNU282987 tended to reduce putative interneuron firing rate in non-stressed rats without changing the activity of projection neurons. This result apparently contradicts data from slice recordings. However, the local BLA inhibitory circuit is formed by a heterogenous population of interneurons and specific neurons can be involved in feedforward or feedback inhibitory circuits (Prager et al., 2016). Furthermore, different populations of interneurons show dissimilar responses to nicotinic agonists. Agonist application elicited a fast-inward response classically related to homomeric α7 nAChR in 12 of 20 interneurons recorded in BLA slices (Pidoplichko et al., 2013). Also, after optogenetic stimulation of basal forebrain projections into the BLA only a specific subpopulation of slow firing interneurons exhibited fast nAChR-dependent EPSPs (Unal et al., 2015). Thus, it is possible that the firing rate reduction observed in our work might be a consequence of the effect on a specific subpopulation of interneurons with a minor role in the control of projection neuron excitability.

4.2. BLA control of VTA DA population activity: role of α7 nAChR

Several brain regions were shown to affect DA neuron population activity in the VTA. Whereas the ventral hippocampus (vHipp)-nucleus accumbens (NAc)-ventral pallidum (VP) circuit exhibits a facilitatory role (Floresco et al., 2003; Lodge and Grace, 2006), the BLA-VP connection has an opposite impact. Pharmacological activation of the BLA reduced the number of spontaneously active VTA DA neurons, an effect dependent on VP activation (Chang and Grace, 2014). Moreover, BLA inactivation reversed the attenuation of DA neuron activity in CMS-exposed rats (Chang and Grace, 2014). In the present study we demonstrated that CMS in fact increases the firing rate of BLA projection neurons, corroborating the proposal that BLA hyperactivity causes impairment in DA

neurotransmission after repeated stress. We also showed that an α7 nAChR full agonist reversed both stress-induced alterations. Thus, it is likely that, in stressed animals, α7 nAChR-induced attenuation of BLA projection neuron firing rate is the leading drive of the normalization of VTA DA tone produced by PNU282987 and may involve the BLA-VP pathway. In contrast, local BLA infusion of PNU282987 increased VTA DA population activity in normal rats (Neves and Grace, 2018). Since BLA inactivation had no effect on VTA DA neurons in non-stressed rats (Chang and Grace, 2014), and in CMS rats there is an inactivation of the vHipp-NAc DA excitatory pathway (Belujon and Grace, 2014), it is possible that BLA activation in the normal rat may activate DA neurons via the BLA-vHipp projection.

Taken together, our findings indicate a potential antidepressant effect for α7 nAChR agonists that is mediated by normalization of BLA hyperactivity and, consequently, of DA hypofunction. Such a mechanism is distinct from those presented by classic antidepressants and points to α7 nAChR as an important target for drug development.

Acknowledgements

References

Andreasen JT, Henningsen K, Bate S, Christiansen S, Wiborg O; 2011 Nicotine reverses anhedonic-like response and cognitive impairment in the rat chronic mild stress model of depression: comparison with sertraline. J. Psychopharmacol 25, 1134–1141. [PubMed: 21169388]

Andreasen JT, Olsen GM, Wiborg O, Redrobe JP; 2009 Antidepressant-like effects of nicotinic acetylcholine receptor antagonists, but not agonists, in the mouse forced swim and mouse tail suspension tests. J. Psychopharmacol 22, 797–804.

Andreasen JT, Redrobe JP; 2009 Antidepressant-like effects of nicotine and mecamylamine in the mouse forced swim and tail suspension tests: role of strain, test and sex. Behav. Pharmacol 20, 286–295. [PubMed: 19404193]

Andreasen JT, Redrobe JP, Nielsen EØ; 2012 Combined α7 nicotinic acetylcholine receptor agonism and partial serotonin transporter inhibition produce antidepressant-like effects in the mouse forced swim and tail suspension tests: a comparison of SSR180711 and PNU282987. Pharmacol. Biochem. Behav 100, 624–629 [PubMed: 22108649]

Arunrungvichian K, Boonyarat C, Fokin VV, Taylor P, Vajragupta O; 2015 Cognitive improvements in a mouse model with substituted 1,2,3-triazole agonists for nicotinic acetylcholine receptors. ACS Chem. Neurosci 6, 1331–1340. [PubMed: 25978789]

Bambico FR, Li Z, Oliveira C, McNeill S, Diwan M, Raymond R, Nobrega JN; 2019 Rostrocaudal subregions of the ventral tegmental area are differentially impacted by chronic stress. Psychopharmacology (Berl). doi: 10.1007/s00213-019-5177-8. [Epub ahead of print]

Belujon P, Grace AA; 2014 Restoring mood balance in depression: ketamine reverses deficit in dopamine-dependent synaptic plasticity. Biol. Psychiatry 76, 927–936. [PubMed: 24931705]

Belujon P, Grace AA; 2017 Dopamine System Dysregulation in Major Depressive Disorders. Int. J. Neuropsychopharmacol 20, 1036–1046. [PubMed: 29106542]

Biala G, Pekala K, Boguszewska-Czubara A, Michalak A, Kruk-Slomka M, Budzynska B; 2017 Behavioral and biochemical interaction between nicotine and chronic unpredictable mild stress in mice. Mol. Neurobiol 54, 904–921. [PubMed: 26780460]

Bodnar AL, Cortes-Burgos LA, Cook KK, Dinh DM, Groppi VE, Hajos M, Higdon NR, Hoffmann WE, Hurst RS, Myers JK, Rogers BN, Wall TM, Wolfe ML, Wong E; 2005 Discovery and structure-activity relationship of quinuclidine benzamides as agonists of alpha7 nicotinic acetylcholine receptors. J. Med. Chem 48, 905–908. [PubMed: 15715459]

Chang C, Grace AA; 2014 Amygdala-ventral pallidum pathway decreases dopamine activity following chronic mild stress in rats. Biol. Psychiatry 76, 223–230. [PubMed: 24209776]

Dagyt G, Den Boer JA, Trentani A; 2011 The cholinergic system and depression. Behav. Brain Res 221, 574–582. [PubMed: 20170685]

Du Y, Grace AA; 2016 Amygdala hyperactivity in MAM model of schizophrenia is normalized by peripubertal diazepam administration. Neuropsychopharmacology 41, 2455–2462. [PubMed: 27000940]

Fales CL, Barch DM, Rundle MM, Mintun MA, Snyder AZ, Cohen JD, Mathews J, Sheline YI; 2008 Altered emotional interference processing in affective and cognitive-control brain circuitry in major depression. Biol. Psychiatry 63, 377–384. [PubMed: 17719567]

Floresco SB, West AR, Ash B, Moore H, Grace AA; 2003 Afferent modulation of dopamine neuron firing differentially regulates tonic and phasic dopamine transmission. Nat. Neurosci 6, 968–973. [PubMed: 12897785]

Furey ML, Drevets WC; 2006 Antidepressant efficacy of the antimuscarinic drug scopolamine: a randomized, placebo-controlled clinical trial. Arch. Gen. Psychiatry 63, 1121–1129. [PubMed: 17015814]

Gill KM, Grace AA; 2013 Differential effects of acute and repeated stress on hippocampus and amygdala inputs to the nucleus accumbens shell. Int. J. Neuropsychopharmacol 16, 2013–2025. [PubMed: 23745764]

Glassman AH, Helzer JE, Covey LS, Cottler LB, Stetner F, Tipp JE, Johnson J; 1990 Smoking, smoking cessation, and major depression. JAMA 264, 1546–1549. [PubMed: 2395194]

Grace AA, Bunney BS; 1983 Intracellular and extracellular electrophysiology of nigral dopaminergic neurons−−1. Identification and characterization. Neuroscience 10, 301–315. [PubMed: 6633863]

Grace AA, Bunney BS; 1984 The control of firing pattern in nigral dopamine neurons: burst firing. J. Neurosci 4, 2877–2890. [PubMed: 6150071]

Hammen C; 2005 Stress and depression. Annu. Rev. Clin. Psychol 1, 293–319. [PubMed: 17716090]

Hannestad JO, Cosgrove KP, DellaGioia NF, Perkins E, Bois F, Bhagwagar Z, Seibyl JP, McClure-Begley TD, Picciotto MR, Esterlis I; 2013 Changes in the cholinergic system between bipolar depression and euthymia as measured with [123I]5IA single photon emission computed tomography. Biol. Psychiatry 74, 768–776. [PubMed: 23773793]

Janowsky DS, Davis JM, El-Yousef MK, Sekerke HJ; 1972 A cholinergic-adrenergic hypothesis of mania and depression. The Lancet 300, 632–635.

Jiang L, Role LW; 2008 Facilitation of cortico-amygdala synapses by nicotine: activity-dependent modulation of glutamatergic transmission. J. Neurophysiol 99, 1988–1999. [PubMed: 18272879]

Klein RC, Yakel JL; 2006 Functional somato-dendritic alpha7-containing nicotinic acetylcholine receptors in the rat basolateral amygdala complex. J. Physiol 576, 865–872. [PubMed: 16931547]

Likhtik E, Pelletier JG, Popescu AT, Paré D; 2006 Identification of basolateral amygdala projection cells and interneurons using extracellular recordings. J. Neurophysiol 96, 3257–3265. [PubMed: 17110739]

Liu ZP, Song C, Wang M, He Y, Xu XB, Pan HQ, Chen WB, Peng WJ, Pan BX; 2014 Chronic stress impairs GABAergic control of amygdala through suppressing the tonic GABAA receptor currents. Mol. Brain 7, 32. [PubMed: 24758222]

Lodge DJ, Grace AA; 2006 The hippocampus modulates dopamine neuron responsivity by regulating the intensity of phasic neuron activation. Neuropsychopharmacology 31, 1356–1361. [PubMed: 16319915]

Lodge DJ, Grace AA; 2012 Divergent activation of ventromedial and ventrolateral dopamine systems in animal models of amphetamine sensitization and schizophrenia. Int. J. Neuropsychopharmacol 15, 69–76. [PubMed: 21329556]

Marcus MM, Björkholm C, Malmerfelt A, Möller A, Påhlsson N, Konradsson-Geuken Å, Feltmann K, Jardemark K, Schilström B, Svensson TH; 2016 Alpha7 nicotinic acetylcholine receptor agonists and PAMs as adjunctive treatment in schizophrenia. An experimental study. Eur. Neuropsychopharmacol 26, 1401–1411 [PubMed: 27474687]

Mark GP, Rada PV, Shors TJ; 1996 Inescapable stress enhances extracellular acetylcholine in the rat hippocampus and prefrontal cortex but not the nucleus accumbens or amygdala. Neuroscience 74, 767–774. [PubMed: 8884772]

Melis M, Scheggi S, Carta G, Madeddu C, Lecca S, Luchicchi A, Cadeddu F, Frau R, Fattore L, Fadda P, Ennas MG, Castelli MP, Fratta W, Schilstrom B, Banni S, De Montis MG, Pistis M; 2013 PPARα regulates cholinergic-driven activity of midbrain dopamine neurons via a novel mechanism involving α7 nicotinic acetylcholine receptors. J. Neurosci 33, 6203–6211. [PubMed: 23554501]

Mineur YS, Fote GM, Blakeman S, Cahuzac EL, Newbold SA, Picciotto MR; 2016 Multiple Nicotinic Acetylcholine Receptor Subtypes in the Mouse Amygdala Regulate Affective Behaviors and Response to Social Stress. Neuropsychopharmacology 41, 1579–1587. [PubMed: 26471256]

Mineur YS, Mose TN, Blakeman S, Picciotto MR; 2018 Hippocampal α7 nicotinic ACh receptors contribute to modulation of depression-like behaviour in C57BL/6J mice. Br. J. Pharmacol 175, 1903–1914. [PubMed: 28264149]

Mineur YS, Obayemi A, Wigestrand MB, Fote GM, Calarco CA, Li AM, Picciotto MR; 2013 Cholinergic signaling in the hippocampus regulates social stress resilience and anxiety-and depression-like behavior. Proc. Natl. Acad. Sci. U S A 110, 3573–3578. [PubMed: 23401542]

Moreines JL, Owrutsky ZL, Grace AA; 2017 Involvement of infralimbic prefrontal cortex but not lateral habenula in dopamine attenuation after chronic mild stress. Neuropsychopharmacology 42, 904–913. [PubMed: 27813530]

Muller JF, Mascagni F, McDonald AJ; 2006 Pyramidal cells of the rat basolateral amygdala: synaptology and innervation by parvalbumin-immunoreactive interneurons. J. Comp. Neurol, 494, 635–650. [PubMed: 16374802]

Neves GA, Grace AA; 2018 α7 Nicotinic receptor-modulating agents reverse the hyperdopaminergic tone in the MAM model of schizophrenia. Neuropsychopharmacology 43, 1712–1720. [PubMed: 29695783]

Ortiz JB, Taylor SB, Hoffman AN, Campbell AN, Lucas LR, Conrad CD; 2015 Sex-specific impairment and recovery of spatial learning following the end of chronic unpredictable restraint stress: potential relevance of limbic GAD. Behav. Brain Res 282, 176–184. [PubMed: 25591480]

Pichat P, Bergis OE, Terranova JP, Urani A, Duarte C, Santucci V, Gueudet C, Voltz C, Steinberg R, Stemmelin J, Oury-Donat F, Avenet P, Griebel G, Scatton B; 2007 SSR180711, a novel selective alpha7 nicotinic receptor partial agonist: (II) efficacy in experimental models predictive of activity against cognitive symptoms of schizophrenia. Neuropsychopharmacology 32, 17–34. [PubMed: 16936709]

Pidoplichko VI, Prager EM, Aroniadou-Anderjaska V, Braga MF; 2013 α7-Containing nicotinic acetylcholine receptors on interneurons of the basolateral amygdala and their role in the regulation of the network excitability. J. Neurophysiol 110, 2358–2369. [PubMed: 24004528]

Porsolt RD, Anton G, Blavet N, Jalfre M; 1978 Behavioural despair in rats: a new model sensitive to antidepressant treatments. Eur. J. Pharmacol 47, 379–391. [PubMed: 204499]

Prager EM, Bergstrom HC, Wynn GH, Braga MF; 2016 The basolateral amygdala γ-aminobutyric acidergic system in health and disease. J. Neurosci. Res 94, 548–567. [PubMed: 26586374]

Rabenstein RL, Caldarone BJ, Picciotto MR; 2006 The nicotinic antagonist mecamylamine has antidepressant-like effects in wild-type but not beta2- or alpha7-nicotinic acetylcholine receptor subunit knockout mice. Psychopharmacology (Berl) 189, 395–401. [PubMed: 17016705]

Rincón-Cortés M, Grace AA; 2017 Sex-Dependent Effects of Stress on Immobility Behavior and VTA Dopamine Neuron Activity: Modulation by Ketamine. Int. J. Neuropsychopharmacol 20, 823–832. [PubMed: 28591782]

Rosenkranz JA, Grace AA; 1999 Modulation of basolateral amygdala neuronal firing and afferent drive by dopamine receptor activation in vivo. J. Neurosci 19, 11027–11039. [PubMed: 10594083]

Rush AJ, Trivedi MH, Wisniewski SR, Nierenberg AA, Stewart JW, Warden D, Niederehe G, Thase ME, Lavori PW, Lebowitz BD, McGrath PJ, Rosenbaum JF, Sackeim HA, Kupfer DJ, Luther J, Fava M; 2006 Acute and longer-term outcomes in depressed outpatients requiring one or several treatment steps: a STAR*D report. Am. J. Psychiatry 163, 1905–1917. [PubMed: 17074942]

Salín-Pascual RJ, Rosas M, Jimenez-Genchi A, Rivera-Meza BL, Delgado-Parra V; 1996 Antidepressant effect of transdermal nicotine patches in nonsmoking patients with major depression. J. Clin. Psychiatry 57, 387–389. [PubMed: 9746444]

Saricicek A, Esterlis I, Maloney KH, Mineur YS, Ruf BM, Muralidharan A, Chen JI, Cosgrove KP, Kerestes R, Ghose S, Tamminga CA, Pittman B, Bois F, Tamagnan G, Seibyl J, Picciotto MR, Staley JK, Bhagwagar Z; 2012 Persistent β2*-nicotinic acetylcholergic receptor dysfunction in major depressive disorder. Am. J. Psychiatry 169, 851–859. [PubMed: 22772158]

Schultz W; 1997 The phasic reward signal of primate dopamine neurons. Advances in Pharmacology 42, 686–690.

Sharp BM; 2017 Basolateral amygdala and stress-induced hyperexcitability affect motivated behaviors and addiction. Transl. Psychiatry 7, e1194. [PubMed: 28786979]

Stedenfeld KA, Clinton SM, Kerman IA, Akil H, Watson SJ, Sved AF; 2011 Noveltyseeking behavior predicts vulnerability in a rodent model of depression. Physiol. Behav 103, 210–216. [PubMed: 21303678]

Steingard RJ, Yurgelun-Todd DA, Hennen J, Moore JC, Moore CM, Vakili K, Young AD, Katic A, Beardslee WR, Renshaw PF; 2000 Increased orbitofrontal cortex levels of choline in depressed adolescents as detected by in vivo proton magnetic resonance spectroscopy. Biol. Psychiatry 48, 1053–1061. [PubMed: 11094138]

Tizabi Y, Overstreet DH, Rezvani AH, Louis VA, Clark E Jr Janowsky DS, Kling MA; 1999 Antidepressant effects of nicotine in an animal model of depression. Psychopharmacology (Berl) 142, 193–199. [PubMed: 10102772]

Tribollet E, Bertrand D, Marguerat A, Raggenbass M; 2004 Comparative distribution of nicotinic receptor subtypes during development, adulthood and aging: an autoradiographic study in the rat brain. Neuroscience 124, 405–420. [PubMed: 14980390]

Tye KM, Mirzabekov JJ, Warden MR, Ferenczi EA, Tsai HC, Finkelstein J, Kim SY, Adhikari A, Thompson KR, Andalman AS, Gunaydin LA, Witten IB, Deisseroth K; 2013 Dopamine neurons modulate neural encoding and expression of depression-related behaviour. Nature 493, 537–541. [PubMed: 23235822]

Unal CT, Pare D, Zaborszky L; 2015 Impact of basal forebrain cholinergic inputs on basolateral amygdala neurons. J. Neurosci 35, 853–863. [PubMed: 25589777]

Ungless MA, Grace AA; 2012 Are you or aren't you? Challenges associated with physiologically identifying dopamine neurons. Trends Neurosci 35, 422–430. [PubMed: 22459161]

Valenti O, Gill KM, Grace AA; 2012 Different stressors produce excitation or inhibition of mesolimbic dopamine neuron activity: Response alteration by stress pre-exposure. Eur. J. Neurosci 35, 1312–1321. [PubMed: 22512259]

Vyas A, Jadhav S, Chattarji S; 2006 Prolonged behavioral stress enhances synaptic connectivity in the basolateral amygdala. Neuroscience 143, 387–393. [PubMed: 16962717]

Willner P; 2016 The chronic mild stress (CMS) model of depression: History, evaluation and usage. Neurobiol. Stress 6, 78–93. [PubMed: 28229111]

Xiao X, Shang X, Zhai B, Zhang H, Zhang T; 2018 Nicotine alleviates chronic stress-induced anxiety and depressive-like behavior and hippocampal neuropathology via regulating autophagy signaling. Neurochem. Int 114,58–70. [PubMed: 29339018]

Zarate CA Jr, Singh JB, Carlson PJ, Brutsche NE, Ameli R, Luckenbaugh DA, Charney DS, Manji HK; 2006 A randomized trial of an N-methyl-D-aspartate antagonist in treatment-resistant major depression. Arch. Gen. Psychiatry 63, 856–864. [PubMed: 16894061]

Zhang W, Rosenkranz JA; 2012 Repeated restraint stress increases basolateral amygdala neuronal activity in an age-dependent manner. Neuroscience 226, 459–474. [PubMed: 22986163]

Zhang W, Rosenkranz JA; 2016 Effects of repeated stress on age-dependent GABAergic regulation of the lateral nucleus of the amygdala. Neuropsychopharmacology 41, 2309–2323. [PubMed: 26924679]

Zhao D, Xu X, Pan L, Zhu W, Fu X, Guo L, Lu Q, Wang J; 2017 Pharmacologic activation of cholinergic alpha7 nicotinic receptors mitigates depressive-like behavior in a mouse model of chronic stress. J. Neuroinflammation 14, 234. [PubMed: 29197398]
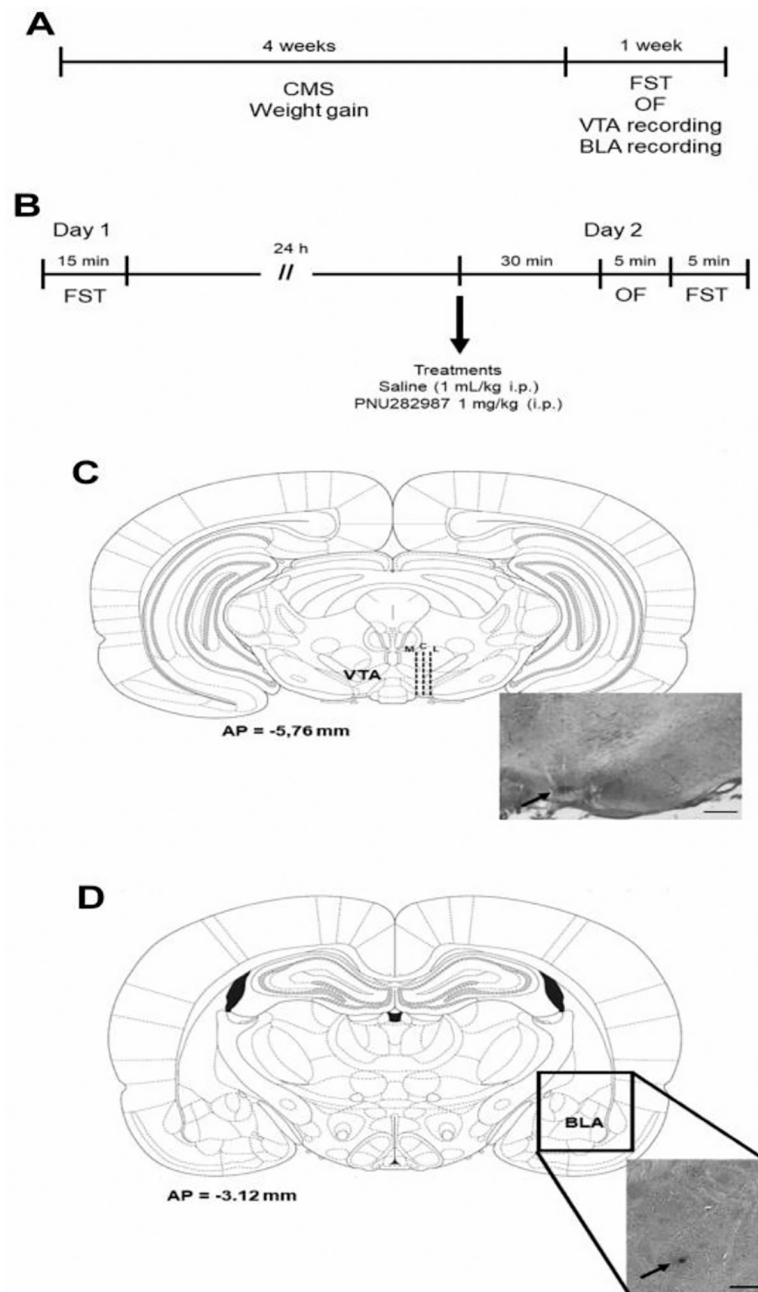
Author Manuscript

Author Manuscript

Author Manuscript

Author Manuscript

Highlights:

- α7 nAChR agonist reverse BLA hyperactivity after CMS

- α7 nAChR agonist normalize VTA DA population activity after CMS

- α7 nAChR agonist shows anti-immobility effect in the CMS model of depression

Fig. 1. Experimental design and histological placement of the electrodes.
(A) Timeline showing the duration of CMS exposure and the period at which the behavioral and electrophysiological assays were conducted. Three different groups of rats were used: behavior (forced swimming test – FST and open-field – OF), VTA and BLA recordings. (B) Timeline of the FST and open field (OF) assays. Histological representation of the electrode placement in the (C) VTA and (D) BLA. Dashed lines represent the electrode tracks. Arrows show the blue dot resulting from Chicago sky blue electrophoretic ejection. M = medial, C = central, L = lateral. Scale bars = 0.5 mm.
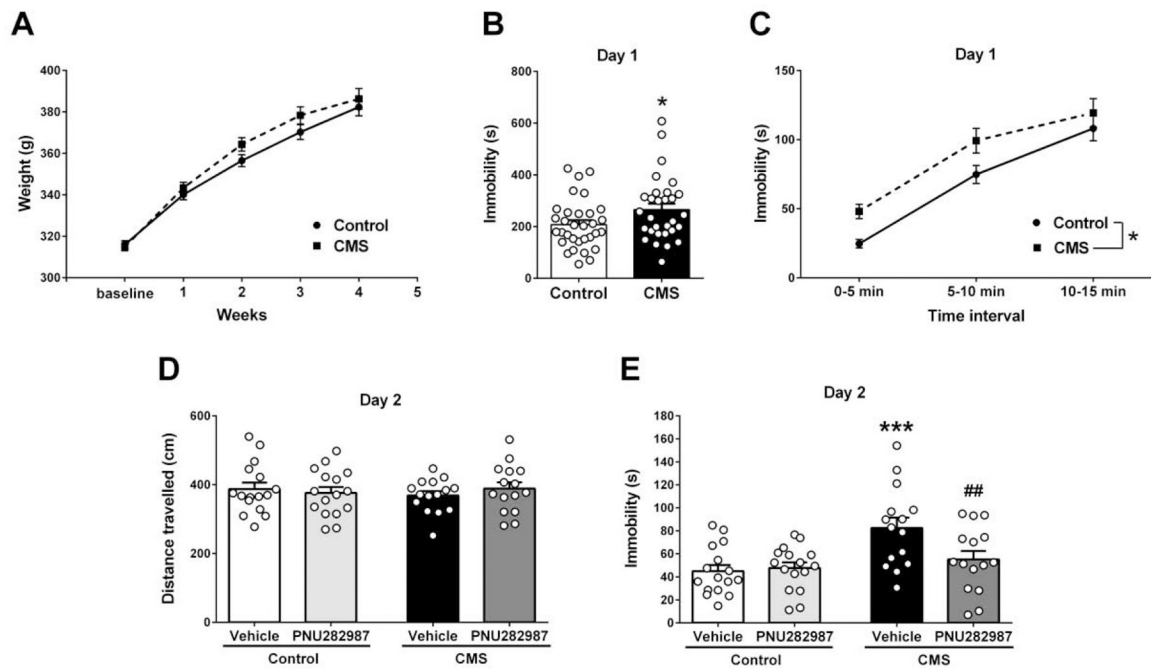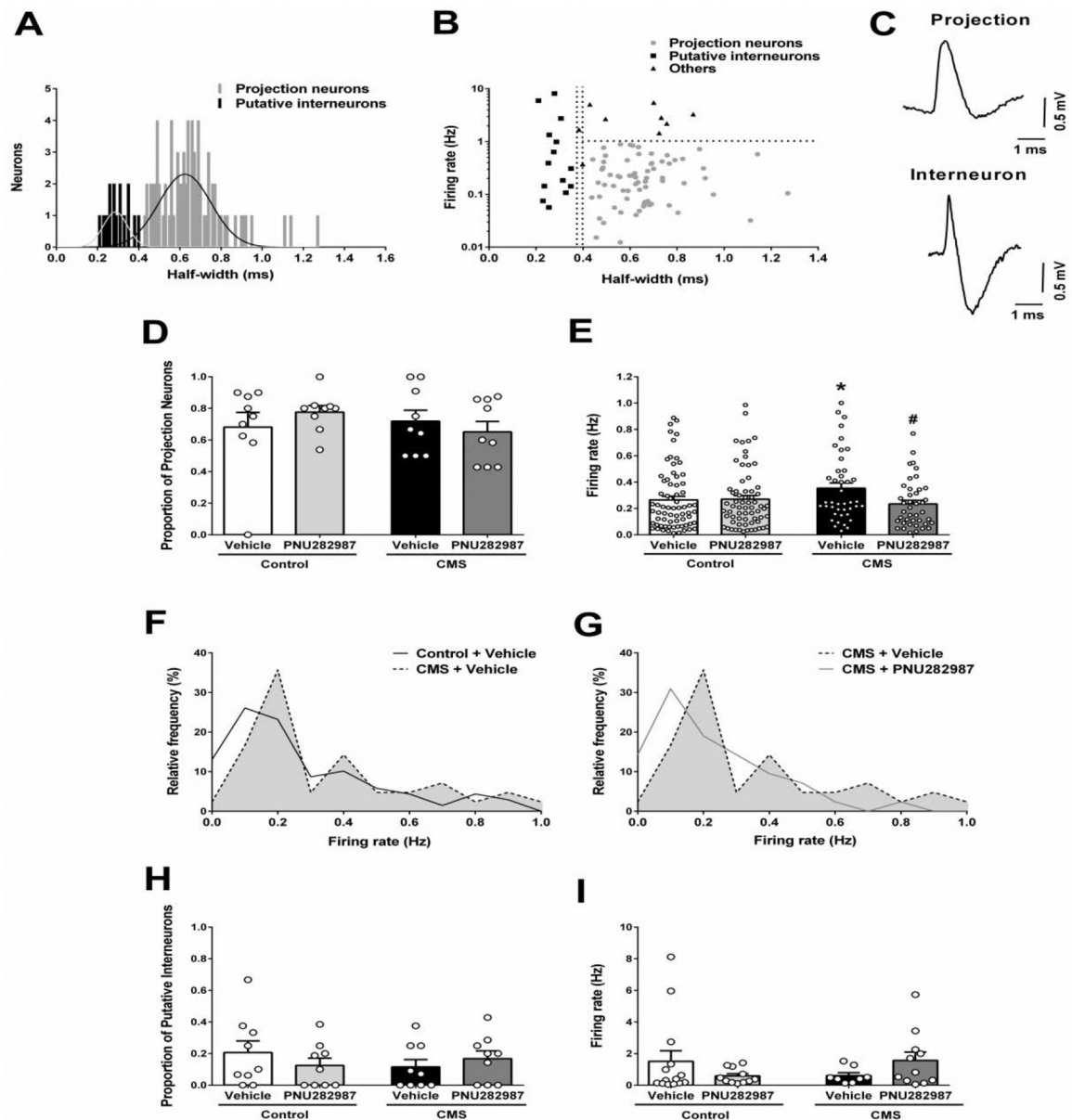
Fig. 2. α7 nAChR full agonist PNU282987 (1 mg/kg i.p.) produced an anti-immobility effect in the FST only in those rats exposed to chronic mild stress.
(A) Body weight of CMS and control rats over the five weeks of experiment (n = 30–32 rats/group). (B) Total immobility time in the first session of forced swim (n = 30–32 rats/group). Students *t* test: *p=0.042. (C) Immobility development across time in the first session of forced swim (n = 30–32 rats/group). Bonferroni post-hoc test: *p=0.038. (D) Total distance travelled (cm) during a 5 min open field task (n=15–16 rats/group). (E) Immobility time in the second forced swim session (n=15–16 rats/group). Bonferroni post-hoc test: ***p<0.001 comparing with control+vehicle, ##p<0.01 comparing with CMS+vehicle. Data are expressed as mean ± S.E.M.
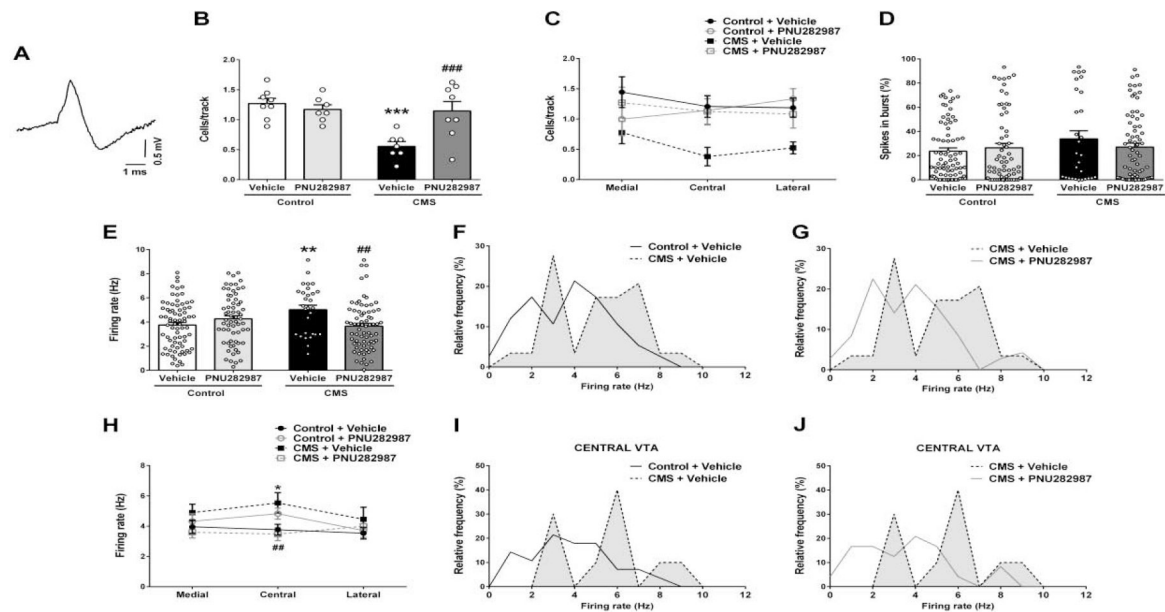
Fig. 3. α7 nAChR full agonist PNU282987 (1 mg/kg i.v.) reversed the stress-induced decrease in dopaminergic neurotransmission.

(A) Representative trace of *in vivo* recorded DA neuron in the VTA. (B) Number of spontaneously active DA neurons recorded per electrode track in VTA (n = 7–8 rats/group). (C) Regional distribution across the VTA of the number of active DA neurons per electrode track (n = 7–8 rats/group). (D) Mean percentage of spikes in bursts and (E) firing rate (Hz) of the recorded DA neurons (n = 29–75 cells/group). Firing rate distribution curves showing (F) the effect of stress and (G) its reversal by PNU282987. Kolmogorov-Smirnov test, control+vehicle vs. CMS+vehicle: p=0.022; CMS+vehicle vs. CMS+PNU282987: p=0.004. (H) Regional distribution across the VTA of average DA neurons firing rate (medial: n = 13–29 cells/group; central: n = 10–28 cells/group; lateral: n = 06–24 cells/group). Firing rate distribution curves showing (I) the effect of stress and (J) its reversal by PNU282987. Kolmogorov-Smirnov test, control+vehicle vs. CMS+vehicle: p=0.092; CMS+vehicle vs. CMS+PNU282987: p=0.066. Data are expressed as mean ± S.E.M. Bonferroni post-hoc test: *p<0.05, **p<0.01, ***p<0.001 comparing with control+vehicle, ##p<0.01, ###p<0.001 comparing with CMS+vehicle.

Fig. 4. α7 nAChR full agonist PNU282987 (1 mg/kg i.v.) counteracts stress-induced BLA hyperactivity.

(A) Distribution of the spike half-width of neurons recorded in the BLA of control+vehicle group (n=92 neurons). Data were best fitted to a sum of two gaussian curves. Extra sum of squares F-test, $F_{(3,123)}$=3.643, p=0.015. (B) Firing rate (Hz) and spike half-width correlation from control+vehicle group neurons showing their distribution between projection neurons, putative interneurons and non-classified (others). (C) Representative traces of putative projection neuron and interneuron recorded *in vivo* in the BLA. (D) Proportion (n=9 rats/ group) and (E) firing rate (n=42–69 neurons/group) of presumptive projection neurons recorded in the BLA. Firing rate distribution curves of the putative projection neurons showing (F) the effect of stress and (G) its reversal by PNU282987. Kolmogorov-Smirnov test, control+vehicle vs. CMS+vehicle: p=0.043; CMS+vehicle vs. CMS+PNU282987:

p=0.073. (H) Proportion (n=9 rats/group) and (I) firing rate (n=08–14 cells/group) of putative interneurons recorded in the BLA. Data are expressed as mean ± S.E.M. Bonferroni post-hoc test: *p<0.05 comparing with control+vehicle, #p<0.05 comparing with CMS +vehicle.